



Proceedings of the Shevchenko Scientific Society. Medical Sciences 2024, 2 (76). <https://doi.org/10.25040/ntsh>

www.mspsss.org.ua

DOI: 10.25040/ntsh2024.02.12

For correspondence: Tetiana Savchuk,
40 V. Hetmana Street, ap. 24; Kyiv,
03058
E-mail: t.savchuk@nmu.ua

Received: 12 Oct, 2024
Accepted: 07 Nov, 2024
Published: 27 Dec, 2024

ORCID IDs

Tetiana Savchuk:
<https://orcid.org/0000-0002-7218-0253>
Tetiana Malysheva:
<https://orcid.org/0000-0003-4071-8327>
Viktoriya Vaslovych:
<https://orcid.org/0000-0002-7503-4745>
Oksana Chernenko:
<https://orcid.org/0000-0001-6292-8339>
Ivan Leshchenko:
<https://orcid.org/0000-0001-8239-256X>
Sergiy Gychka:
<https://orcid.org/0000-0001-6292-8339>

Disclosures: The authors declared no conflict of interest.

Author Contributions:

Conceptualization: Tetiana Savchuk, Tetiana Malysheva, Viktoriya Vaslovych, Oksana Chernenko, Ivan Leshchenko, Sergiy Gychka;

Writing: Tetiana Savchuk, Tetiana Malysheva, Viktoriya Vaslovych, Oksana Chernenko, Ivan Leshchenko, Sergiy Gychka;

Review & editing: Tetiana Savchuk, Tetiana Malysheva, Viktoriya Vaslovych, Oksana Chernenko, Ivan Leshchenko, Sergiy Gychka.

Ethical approval: The Bioethics Committee of the Bogomolets National Medical University, protocol No. 144 of March 29, 2021.

Funding: The authors received no financial support for their study.



© All authors, 2024

Original research: Clinical sciences

PATHOMORPHOLOGICAL CHANGES OF THE PLACENTA IN THE ACUTE PERIOD OF CORONAVIRUS DISEASE 2019 (COVID-19) AT 37–41 WEEKS OF GESTATION

Tetiana Savchuk¹, Tetiana Malysheva², Viktoriya Vaslovych², Oksana Chernenko², Ivan Leshchenko³, Sergiy Gychka¹

¹Department of Pathological Anatomy, Bogomolets National Medical University, Kyiv, Ukraine

²Department of Neuropathomorphology with Laboratories (pathological, electron microscopy, tissue culture), State Institution “Romodanov Neurosurgery Institute of the National Academy of Medical Sciences of Ukraine”, Kyiv, Ukraine

³Department of Physiology, Bogomolets National Medical University, Kyiv, Ukraine

Introduction: Coronavirus disease 2019 (COVID-19) is a risk factor for developing placental dysfunction when a pregnant woman is infected before 35 weeks of gestation. According to our previous studies, no cases of antenatal asphyxia were observed when infection occurred after this gestational age. The children were born with high Apgar scores and negative PCR tests for SARS-CoV-2 RNA from women who had clinical manifestations of COVID-19 confirmed by a positive PCR test.

Objective of the Study: To investigate the pathomorphological changes in the placenta during full-term pregnancy in the acute phase of COVID-19 in women.

Materials and Methods: The placenta (n=37) was studied at the birth of a live full-term fetus (main group) and compared to placentas from physiological deliveries before the COVID-19 pandemic (n=38, comparison group). Comprehensive morphological methods were used, including macroscopic, microscopic, immunohistochemical, electron-microscopic, morphometric, and statistical.

Results: Structural changes were noted in the syncytiotrophoblast of the placenta, including loss of microvilli, nuclear membrane invaginations, appearance of cytoplasmic vacuoles, apoptosis, and chromatin condensation. In the endothelium, apoptosis, swelling, and mitochondrial homogenization were observed. Spherical structures similar to viral particles with an electron-dense membrane were found extracellularly, outside the fibroblast. The structural features indicated endothelial dysfunction and circulatory disorders – 97.3% (95% CI: 89.4%–100%); placentitis – 100% (95% CI: 94.6%–99.5%). Swelling of the chorionic villi was observed in 97.3% (95% CI: 89.4%–100%), with the percentage of stroma in the terminal villi increasing to 71.1 [49.5; 85.1] compared to 32.6 [26.2; 39.5] in the comparison group (p < 0.0001). A reduction in the percentage of vessels in the terminal villi was noted due to a decrease in lumen size – 29.9 [14.5; 51.2] compared to 67.4 [58.7; 73.8] in the comparison group (p < 0.0001); and a reduction in the percentage of the intervillous space to 21.7 [12.9; 33.1] compared to 44.2 [40.3; 49.7] (p < 0.0001).

Conclusions. In the acute phase of COVID-19, pathomorphological changes were observed in the placenta, indicating endothelial dysfunction caused by SARS-CoV-2. This was manifested by circulatory disorders, swelling of the stroma of the chorionic villi with a reduction in capillary lumen size and the percentage of free intervillous space, and inflammatory infiltration, leading to maternal and fetal malperfusion in the placenta. In our opinion, pathology changes in the structures forming the vasculosyncytial membranes were compensated by the already-formed placenta with sufficient terminal villi and local placentitis (limited to one cotyledon). Apoptotic changes in the syncytiotrophoblast and endothelium are morphological manifestations of hypoxia and energy deficiency in the placenta. These changes require further investigation in the context of the prolonged post-COVID interval in pregnant women infected with the SARS-CoV-2 virus during the second trimester.

Keywords: placenta, COVID-19, SARS-CoV-2, pregnancy, chorionic villi, pathology

Introduction

The placenta in a full-term pregnancy is represented by cotyledons, which accommodate the branching of one stem villus into mature intermediate and terminal villi of the chorion [1]. The formation of terminal villi occurs in the third trimester of pregnancy; they are the source of the formation of vasculosyncytial membranes [2]. The latter provide diffusional exchange and are formed by an endotheliocyte, a basal membrane and the syncytiotrophoblast cytoplasm [3]. The satisfactory condition of the fetus is ensured by sufficient vascularization of the terminal villi of the chorion and the free intervillous space (IS) [4, 5, 6, 7], which is a prerequisite for adequate placental perfusion [8, 9]. Cases of intrauterine infection of the fetus and antenatal death of the fetus up to the 35th week of pregnancy were described, which were explained by the formation of placental dysfunction with COVID-19 in a pregnant woman [10, 11, 12, 13].

One of the effects of SARS-CoV-2, the causative agent of coronavirus infection (COVID-19), is binding to the receptor for angiotensin-converting enzyme type II (ACE2), which is present in the cells of many organs [14, 15], resulting in the activation of endothelial cells, macrophages, neutrophils that leads to impaired microcirculation and remodeling of vessels of the villous chorion [16, 17]. Determining individual components of compensatory mechanisms of the placenta, which is the key to the birth of PCR-negative babies in women with COVID-19 after 36 weeks of pregnancy, prompted us to conduct a study.

The purpose of the study: To investigate the pathomorphological changes in the placenta during full-term pregnancy in the acute phase of COVID-19 in women.

Research materials and methods

We studied the placenta (n=37) in the acute phase of COVID-19 in pregnant women who gave birth to live full-term infants at 37–41 weeks of gestation. The material was selected from the Department of Pathological Anatomy of the NSCH OHMATDYT of the Ministry of Health of Ukraine from 2020 to 2021. COVID-19 in pregnant women was confirmed by a positive polymerase chain reaction (PCR) result for the presence of SARS-CoV-2 RNA. The PCR test of newborns was negative. The post-covid interval (the period from the diagnosis of COVID-19 to delivery) was between 1 and 4 weeks. To compare the data, placentas (n=38) were studied during physiological childbirth before the COVID-19 epidemic. Macroscopic, microscopic, electron-microscopic (EM), morphometric and statistical research methods were used. Sections were stained histologically using generally accepted methods and immunohistochemically using monoclonal mouse antibodies against CD34 (Thermo Fisher Scientific, USA) in working dilutions. To visualize a complete histological tissue section, a computer study of the digitized slides was performed using a Panoramic DESK DW II digital scanner [18]. To determine the quantitative differences between terminal villi (capillaries, stroma) and IS in the graphic editor Microsoft Paint, the studied histological structures were additionally colored in a color that differed from the colors of the histological staining of the structures in the photo (capillaries – in black, background – in green) with subsequent loading of archival images (×200, ×600) in JPEG format using ONLINE JPG TOOLS service (onlinejpgtools.com/find-dominant-jpg-colors) with the determination of the color percentage. The percentage of color represents the percentage of the area of the studied structure in the photo [5, 7]. The density of syncytial nodules was calculated using quantitative planimetry [19]. Ultrastructural changes in vasculosyncytial membranes were studied using EM.

Placental tissue fragments with a size of 1–2 sq. mm were taken immediately after delivery, fixed in a mixture of 4% paraformaldehyde (Aldrich, Germany), 2.5% glutaraldehyde (Raaral, Hungary) and 0.1 M cacodylate buffer pH 7.4 ("Agar scientific," Germany) followed by fixation in a 1% solution of osmium tetroxide ("Agar scientific," Germany) [20]. The samples were dehydrated in increasing concentrations of ethanol and oxypropylene and embedded in a mixture of epoxy resins (Epon-Araldite, "Fluka," Switzerland) using standard electron microscopy techniques. Ultrathin sections with a thickness of 70 nm were made on an LKB ultratome (Sweden). To increase the contrast, they were stained using the standard Reynolds method [21] and viewed through an electron microscope PEM 100-1 ("SELM," Ukraine) at an accelerating voltage of 75 kV.

Statistical analysis of the results was performed using the STATISTICA 8.0 software package (StatSoft, USA), serial number STA862D175437Q, and MedStat, serial number 85684586. Variational statistics methods were used for statistical data processing. The non-parametric Mann-Whitney U Test was used to assess the difference between the average values of two independent populations with small samples. Rank data are presented in median format with lower and upper quartiles (Me [Q1; Q3]). Differences were considered statistically significant at $p < 0.05$.

The results

We studied pathomorphological changes in the placentas of babies born alive to mothers who had COVID-19 at 36–40 weeks of pregnancy. The course of the coronavirus disease in 14 pregnant women was defined as mild, in 21 – medium-severe, and in 2 cases, a severe condition with pneumonia was diagnosed. Despite the severity of the mother's illness, children were assessed at birth as having 7–9 points on the Apgar scale and a negative PCR test for the presence of RNA of the SARS-CoV-2 virus.

At the time of delivery, the gestation period was 39.9 [36. 41] weeks (Table 1) and did not differ from the period in the comparison group, which was 39.4 [37. 40] weeks.

During the macroscopic examination of the placentas with COVID-19, dyscirculatory disorders were revealed: uneven, full blood (Fig. 1) and focal hemorrhages in the thickness of the organ (Fig. 1.F). On the maternal surface, yellowish deposits – fibrin (Fig. 1. B. C) and blood clots (Fig. 1. B. E). The dark cherry color of the blood attracted attention. The amniotic membranes were thickened and yellowish, with focal hemorrhages (Fig. 1. A, D). Focal infarcts of red and pale-yellow color were found under the membranes and on the section of the placenta in 29.7% (95% CI: 15.9%-45.8%) (Fig. 1. D, F).

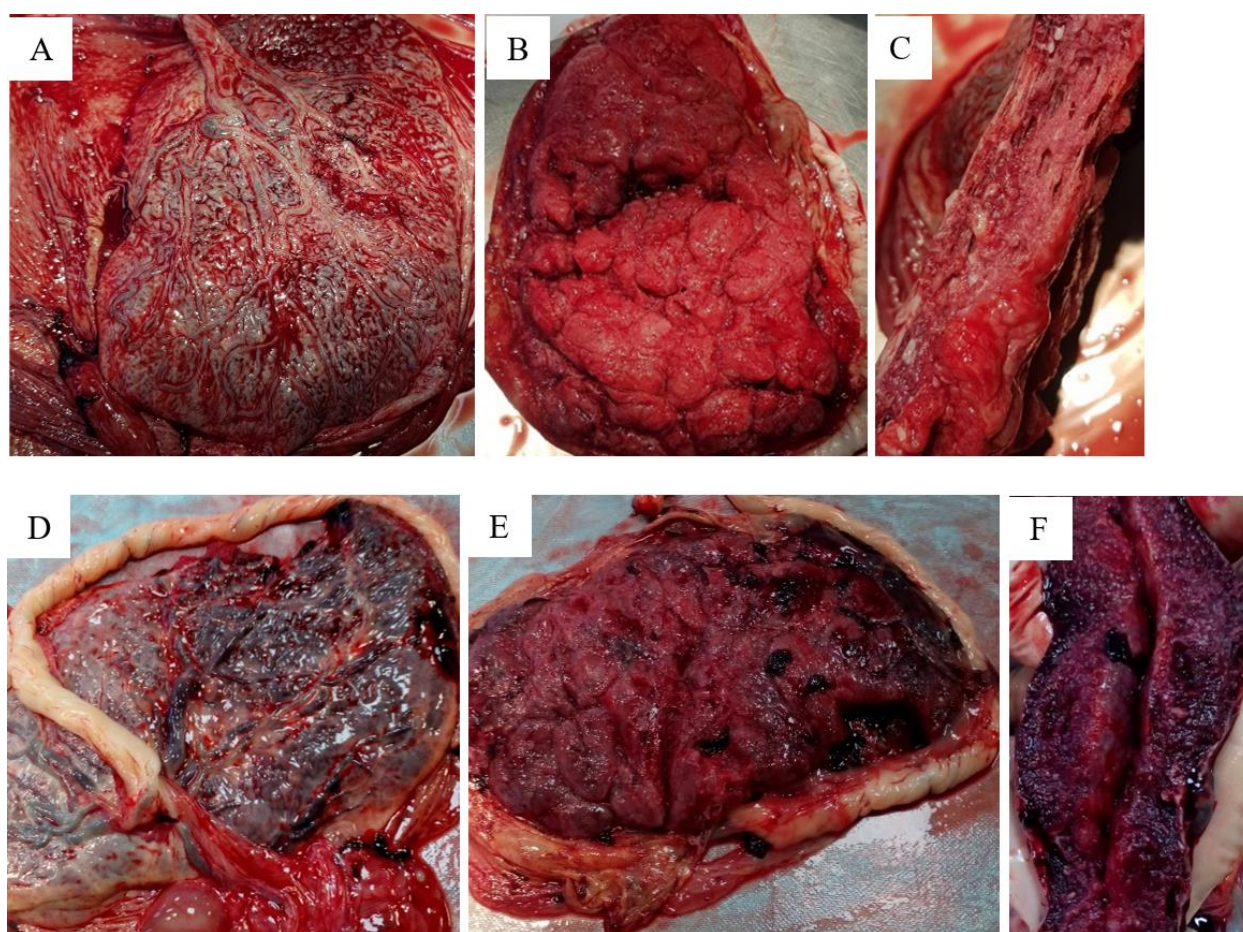


Figure 1. Pathomorphological changes in the placenta in a 39-week pregnant woman with COVID-19 who gave birth to a live fetus. **A, B, C** – mild case; **D, E, F** – severe condition with pneumonia. **A, D** – fetal surface. **B, E** – maternal surface. **C, F** – view of the placenta in cross-section

During the microscopic examination of the placentas of pregnant women with COVID-19, dyscirculatory disorders were detected in 97.3% (95%CI: 89.4%-100%) of cases in the acute phase of the disease (Fig. 2. A; Table 1): hemorrhages in the IS (Fig. 4) were identified by EM as aggregation (clumping) of erythrocytes (Fig. 4. E – 1). Stasis and thrombosis were observed in the lumen of the chorionic villi vessels (Table 1). During EM, erythrocyte aggregation with the formation of specific columns (Fig. 5. D, F, H – 1) and platelet degranulation (Fig. 5. F – 2) were detected in the vessel

lumen. Apoptotic changes were noted in the endothelium of vessels: condensation of chromatin, intussusception of the nuclear envelope, and formation of numerous cytoplasmic processes (Fig. 5. I). All observations were accompanied by placentitis: basal deciduitis in 100% (95%CI: 94.6–99.5%), chorioamnionitis in 97.3% (95%CI: 89.4%-100%) and focal intervillitis in 16.2% (95%CI: 6.0–30.1%) of cases. Intervillitis was manifested by leukocyte infiltration in the IS and was accompanied by fibrinoid deposition along the perimeter of the chorionic villi (Fig. 2 B; Fig. 4 B, C) with partial loss of the syncytiotrophoblast layer (Fig. 3. A; Fig. 4. B, C). The compaction of the nucleus (karyopyknosis) in the form of chromatin condensation (Fig. 4. D. 4; A; Fig. 6. B, D) was observed in the cells of the preserved syncytium, and an expansion of smooth endoplasmic reticulum cisterns with the formation of numerous vacuoles was observed in the cytoplasm (Fig. 4 G, D.; Fig. 5 D).

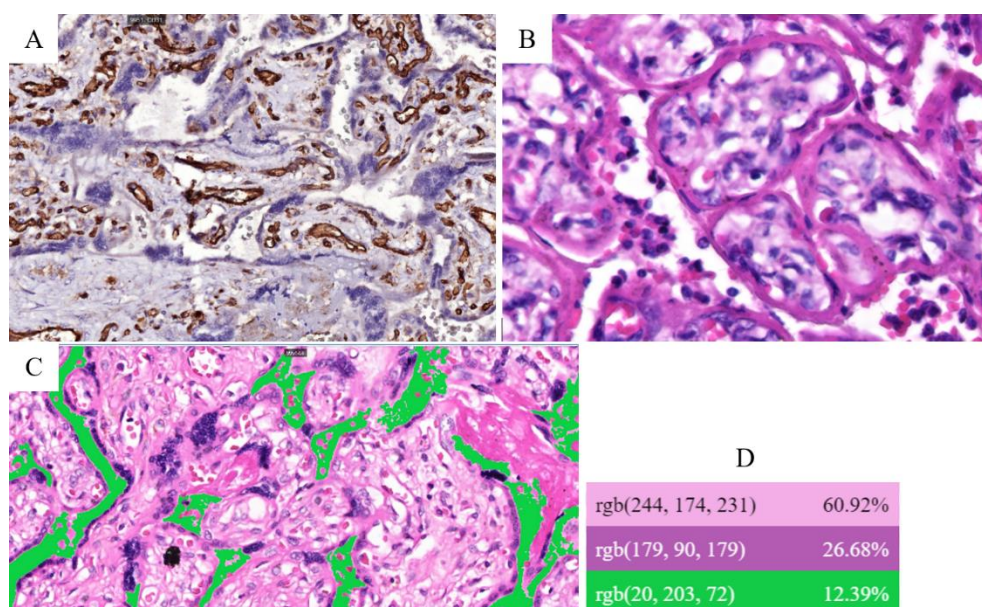


Figure 2. Structural changes of the placenta in the acute phase of COVID-19 in a pregnant woman: **A** – COVID-19 at 39 weeks of gestation. An increase in the number of syncytial nodules and erythrocytes in IS; expression of monoclonal antibodies against CD34 in the endothelium of arterioles of chorionic villi, $\times 400$. **B** – COVID-19 at 38 weeks of gestation. Villi are outlined by fibrinoid and leukocytes in IS; H&E stain, $\times 600$. **C** – quantitative determination of IS according to the aforementioned method; H&E stain, $\times 400$. **D** – determination of the percentage of chorionic villi and IS in the ONLINE JPG TOOLS service

The number of terminal villi of the chorion did not differ from the comparison group, amounting to 25.9 [21; 29] versus 25.3 [20; 30]. However, in 97.3% (95% CI: 89.4–100%) of cases with COVID-19 in the mother, the terminal villi of the chorion appeared swollen (Fig. 3. A.1.2.3; Fig. 5. A, C, E, G) compared to the control group (Fig. 3. B.1.2.3). Spherical structures resembling viral particles [15] with an electron-dense shell, were detected (Fig. 5. G – arrows). These spherical particles were located externally, near the cell membrane of the fibroblast. Electron microscopy revealed mucoid changes in the ground substance of the connective tissue of the stroma of the chorionic villi, characterized by the loss of collagen fiber compactness, while the fiber structure remained intact. Fibrinoid changes were also observed, with the loss of transverse striation, homogenization, and disintegration (Fig. 5. C, E). Fibrin deposition in the stroma was also noted. The percentage of stroma in terminal villi in COVID-19 cases was 71.1 [49.5; 85.1] against 32.6 [26.2; 39.5] in the comparison group ($p < 0.0001$). There was also a decrease in the percentage of the lumen area of the vessels in the terminal villi – 29.9 [14.5; 51.2] (Fig. 3. A. 1. 2. 3) against 67.4 [58.7; 73.8] in the comparison group; $p < 0.0001$ (Fig. 3. B. 1. 2. 3). A decrease in the percentage of IS was observed – 21.7 [12.9; 33.1] compared to 44.2 [40.3; 49.7], $p < 0.0001$ (Fig. 2. C. D.). An increase in the number of syncytial nodules was observed between closely located terminal villi (Fig. 6), amounting to 12.8 [11; 14] in COVID-19 cases versus 5.9 [5; 7] in the comparison group. Under EM, the nodules appeared as clusters of irregularly shaped syncytiotrophoblast nuclei, with numerous protrusions of the nuclear envelope, nucleoli disorganization, and chromatin condensation (Fig. 6. B). In areas where the terminal villi were closely positioned, a reduction in the number of microvilli on the syncytiotrophoblast surface, changes in their shape, and a decrease in the

length of individual villi until their complete loss were observed (Fig. 6. D. 2). Similar microvilli alterations were detected when the villi came into contact with erythrocytes during hemorrhages in the IS (Fig. 4.D).

Table 1. Pathomorphological changes in the placenta of live infants born to mothers with COVID-19 during the acute phase, compared to a control group

Pathomorphological changes		COVID-19 (n=37)	Comparison group (n=38)
Pregnancy period		39.9 [36; 41]	39.4 [37; 40]
Number of terminal villi ¹		25.9 [21; 29]	25.3 [20; 30]
Swelling of the stroma of terminal villi, percentage of stroma		n=36 97.3% (95%IS: 89.4–100%); 71.1[49.5; 85.1]*	n=0 0% (95%IS: 0.0–4.7%); 32.6 [26.2; 39.5]
Stasis, thrombosis, hemorrhages		n=36 97.3% (95%IS: 89.4%-100%)*	n=4 10.5% (95%IS: 2.7–22.5%)
Narrowing of lumen of capillaries of terminal villi, percentage of capillaries		n=36 97.3% (95%IS: 89.4–100%); 29.9 [14.5; 51.2]*	n=0 0% (95%IS: 0.0–4.7%); 67.4 [58.7; 73.8]
Placental lesions	Chorioamnionitis	n=36 97.3% (95%IS: 89.4–100%)	–
	Intervillositis	n=6 16.2% (95%IS: 6.0–30.1%)	
	Basal deciduitis	n=37 100% (95%IS: 94.6–99.5%)	
Infarction		n=11 29.7% (95%IS: 15.9–45.8%)	n=5 13.2% (95%IS: 4.2–26%)
Syncytial nodules ¹		12.8 [11; 14]*	5.9 [5; 7]
Intervillous space		21.7 [12.9; 33.1]*	44.2 [40.3; 49.7]

Note: 1 – the number of studied structures in a single field of view at a microscope magnification of 400x; *p<0.0001 (Mann-Whitney U-test)

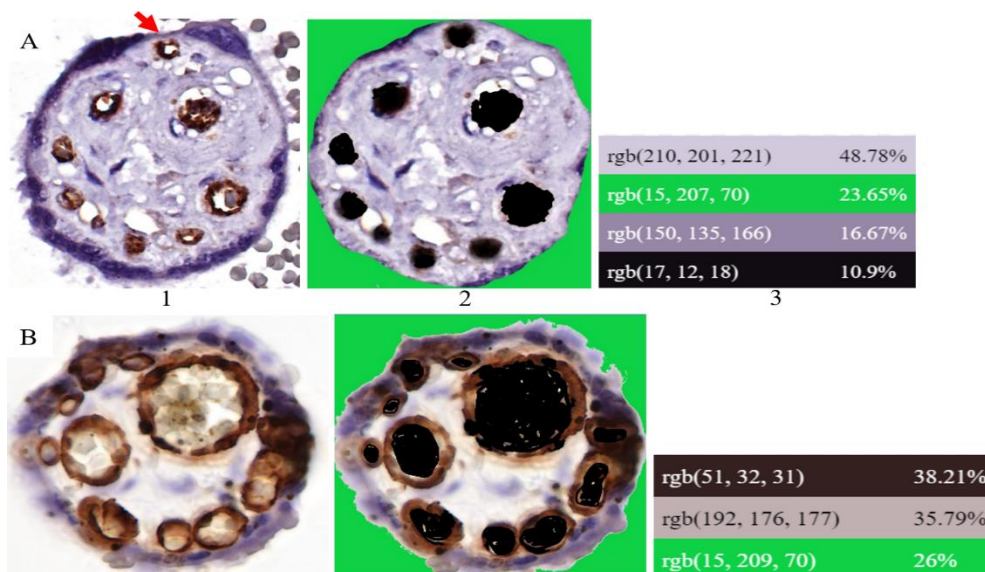


Figure 3. Microscopic changes of placentas in COVID-19 (A) and the control group (B). Quantitative determination of the percentage ratio of blood vessels and stroma in a histological section of terminal villi in a pregnant woman with COVID-19 compared to physiological childbirth: 1 (A, B) – terminal villi, expression of monoclonal antibodies against CD34 in the endothelium of chorionic villi vessels, (A, $\times 700$; B, $\times 1000$). 2 – using the graphic editor Microsoft Paint, the lumen of the blood vessels and the surrounding background of the villi were colored (black and green). 3 – determination of the percentage of vessels and stroma was carried out according to the method described above

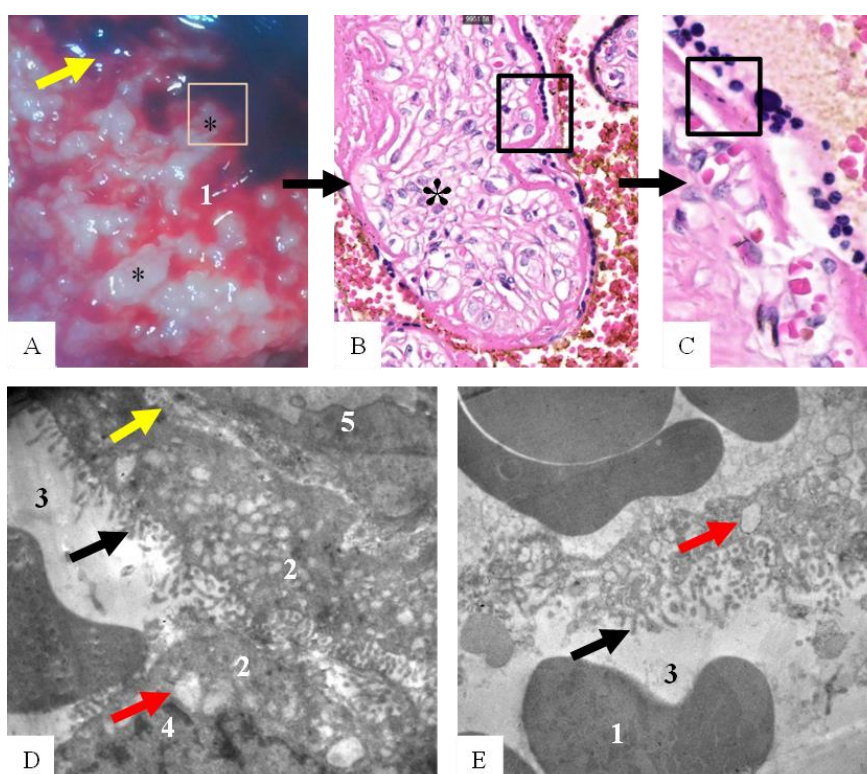


Figure 4. Multilevel: macroscopic, microscopic, and electron-microscopic changes in the placenta during COVID-19 in a pregnant woman in the acute phase of the disease. A – hemorrhages (yellow arrow) between the villi of the chorion (*), $\times 5$. B – swelling of the terminal villus surrounded by fibrinoid, partial loss of the syncytiotrophoblast layer, and erythrocytes in the IS. D, E – erythrocytes (1) in IS (3); D – reduction of the distance between terminal villi (2), parietal condensation of chromatin in the syncytiotrophoblast nucleus (4), syncytiotrophoblast microvilli (black arrow), vacuoles in the syncytiotrophoblast cytoplasm (red arrow), vessel (5), and expansion of the basement membrane (yellow arrow), B, C – H&E; $\times 400$; $\times 1100$; D, E, – EM, $\times 4000$, $\times 6000$

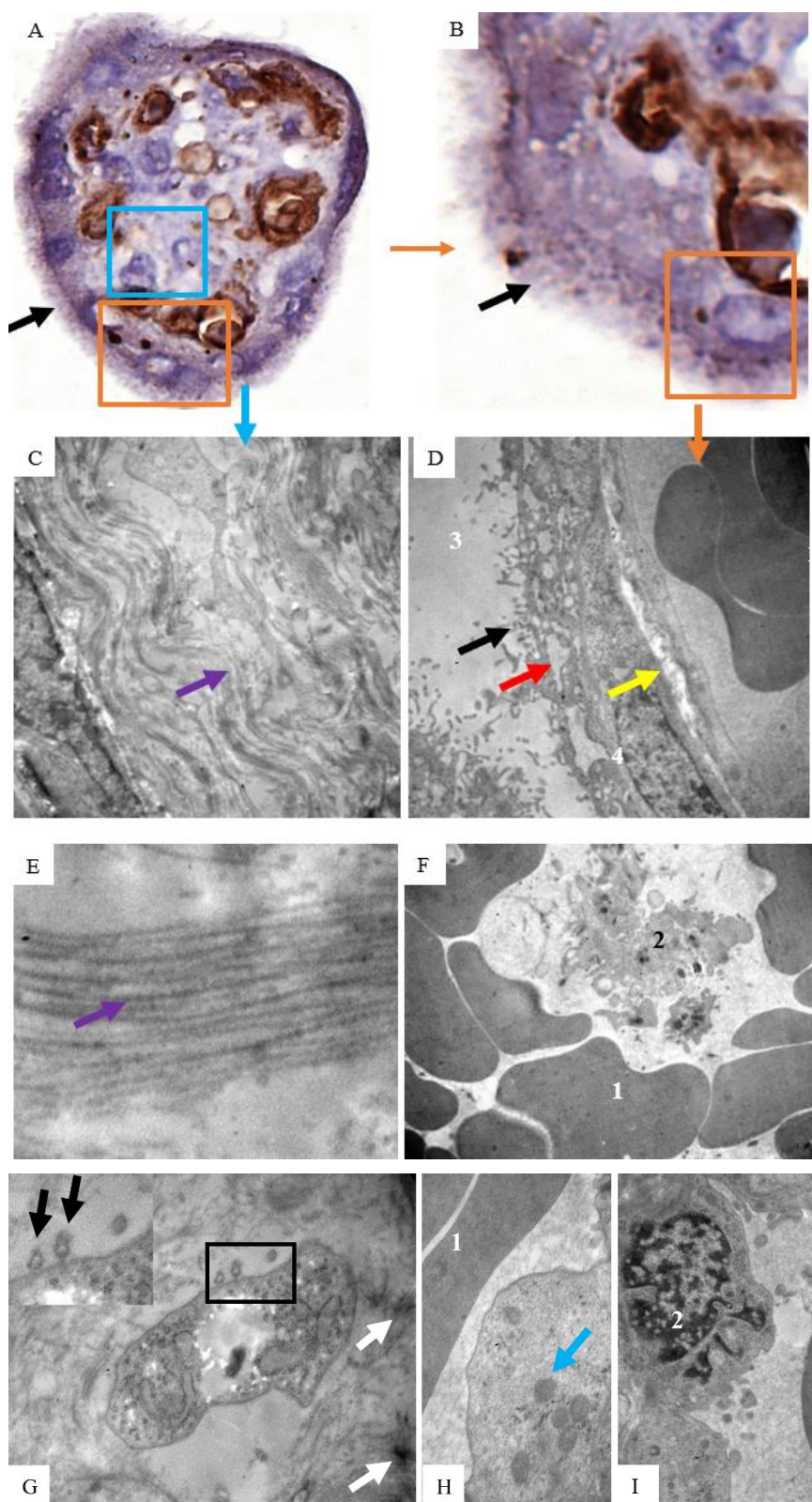


Figure 5. Microscopic and electron-microscopic changes in the placenta during COVID-19 in a pregnant woman in the acute phase of the disease. **A, B** – terminal villus of the chorion, stroma (blue square), vasculo-syncytial membrane (brown color); microvilli (black arrow); CD34, $\times 1100$, $\times 2000$. **C, E** – swelling of the villus stroma, collagen fibers (purple arrow); **G** – viral particles (black arrow); fibrinoid swelling of collagen fibers, fibrin (white arrow). **D** – microvilli (black arrow), vacuoles (red arrow), expansion of the basement membrane (yellow arrow). **F** – aggregation of erythrocytes (1) and platelet degranulation (2) in the vessel lumen. **H** – clumping of erythrocytes (1) in the vessel lumen; mitochondria in the endotheliocyte cytoplasm (blue arrow). **I** – erythrocyte (1) in the vessel lumen, endotheliocyte (2). **C, F, I** – EM, $\times 3000$; **D, E, G, H** – EM, $\times 10000$

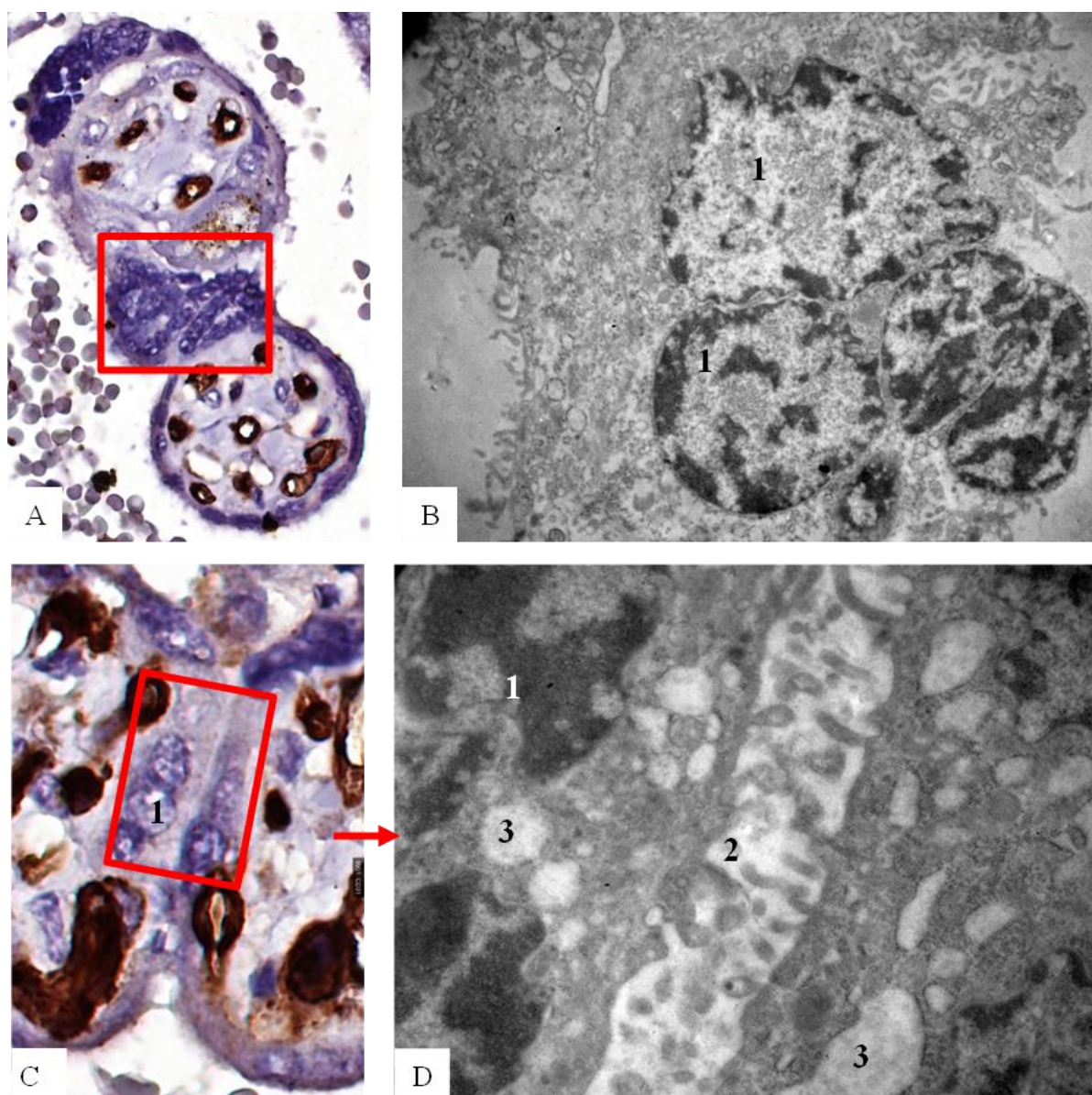


Figure 6. Microscopic and electron microscopic changes in the placenta during COVID-19 in a pregnant woman in the acute phase of the disease. A, C – CD34, $\times 950$; $\times 2000$; B, D – EM, $\times 3000$, $\times 10000$. B.1 – changes in syncytiotrophoblast nuclei, nuclear fragmentation (arrow). D.1 – changes in the syncytiotrophoblast nucleus (apoptosis); 2 – microvilli on the surface of the terminal villus of the chorion; 3 – cytoplasmic vacuoles

Discussion

The identified pathomorphological changes of the placenta in the acute phase of COVID-19 revealed several features. The gestational age at delivery was 39.9 [36, 41] weeks. Despite the severity of the mother's illness, the children were born with negative PCR tests and high Apgar scores. We did not find a statistically significant difference in the studied cases between the severity of COVID-19 in a pregnant woman and the morphological changes in the placenta. The literature presents conflicting data regarding the relationship between the severity of the disease in the mother and the fetus's condition at birth [3, 11, 26]. Some authors identified a correlation between the severity of the disease in a pregnant woman and changes in the placenta but did not take into account the period of gestation during which the woman became ill [22]. In previous studies, we established that the severity of the condition of the fetus and newborn (as estimated according to the Apgar scale of 3–6 points) is associated with the severity of inflammatory changes in the

placenta, which were mainly observed with COVID-19 in women in the second trimester of pregnancy [7, 11, 13]. This was explained by the inability of the protective mechanisms of the immature placenta [5, 17].

Pathomorphological manifestations in the placenta associated with COVID-19 in the acute phase of the illness in the mother were placentitis (chorioamnionitis – 97.3% (95%CI: 89.4–100%), intervillitis – 16.2% (95%CI: 6.0–30.1%), basal decidualitis – 100% (95%CI: 94.6–99.5%)), which indicates the exudation phase of the inflammatory process. At the same time, the intensity of leukocyte infiltration in the membranes and the basal plate of the placenta was usually moderate. Confirmation of the vertical route of infection with the SARS-CoV-2 virus is the greater severity of basal decidualitis and subchorionic intervillitis than the severity of inflammation in the amniotic membranes [5]. We noted that the prevalence of intervillitis in full-term pregnancy was confined to a single, already-formed cotyledon. Other researchers have noted villitis and fibrinoid deposition in the intervillous space in 37.7% of observations [23]. The formation of fibrinoid around the chorionic villi (between the villous stroma and the layer of syncytiotrophoblast (Fig. 4B) is associated with increased permeability of cell membranes. EM changes in the syncytiotrophoblast were characterized as apoptotic: chromatin condensation, the appearance of cytoplasmic vacuoles, and loss of microvilli. Factors that activate apoptosis in COVID-19 are cytokine storm and tissue hypoxia [24]. The appearance of apoptotically changed cells, both syncytiotrophoblast and endothelium, indicates an energy deficiency of the latter. In areas of the placenta where the villi are outlined by fibrinoid (Fig. 4. C), perfusion is disturbed, which is one of the stages of forming placental insufficiency. According to other specialists, generalized intervillitis, the development of which is caused by still unformed cotyledons in the case of a premature placenta, can be the cause of the antenatal death of the fetus [7, 11]. Dyscirculatory disorders (hemorrhages in the IS) and the appearance of fibrinoid in the IS reduce its percentage of the latter up to complete obliteration, which is normally represented by winding channels between the chorionic villi [6, 8, 9]. Thus, the factor that ensures adequate maternal perfusion is free IS. Fetal perfusion was affected not only by apoptotic changes in the endothelium of vessels and cytoplasm (condensation of chromatin, intussusception of the nuclear membrane, swelling of mitochondria) but also by the dyschemic changes we discovered (stasis, thrombosis in the lumen of vessels). In our study, we primarily focused on changes in the distal parts of the villous chorion, as vasculosyncytial membranes are formed in the terminal chorionic villi. Normally, the thickness of the latter decreases to 1–2 μm due to the protrusion of fetal capillaries into the syncytiotrophoblast layer [2]. Lateral displacement of the syncytiotrophoblast layer is observed in areas of vessel protrusion (Fig. 3. A. 1 – red arrow). An increase in the thickness of vasculosyncytial membranes due to the density of the syncytiotrophoblast layer initiates the death of the latter's cells. It leads to pathological activation of the endothelium as described by scientists in preeclampsia. A similar mechanism of development is the basis of the preeclampsia-like syndrome described by scientists in the case of coronavirus disease in the mother and is caused by the direct effect of the virus on endotheliocytes (aponecrosis – according to Sankar K., 2012), or by the effect of cytokines stimulated by SARS-CoV-2 [3]. According to researchers, substances produced by activated endothelial cells were delivered both into the vascular lumen, leading to microcirculation disturbances, and subendothelially, affecting smooth muscle cells and fibroblasts [25]. This was confirmed by the authors' evidence of proliferative changes in the muscle layer of the arterioles of the trunk and intermediate villi of the chorion with subsequent fibrosis and an increase in the post-COVID interval [12, 13]. In our observations, similar changes in the vessel wall did not have time to form due to the short duration of the post-COVID interval (1–4 weeks). Dysfunction of the endothelium led to impaired microcirculation, vasoconstriction, and tissue swelling. In our observations, between villi outlined by fibrinoid and swollen terminal villi, an increase in the number of syncytial nodules up to 12.8 was noted [11; 14] against 5.9 [5; 7] in the comparison group; $p < 0.0001$. This increase is likely a compensatory mechanism to create more space between the villi to restore adequate microcirculation. According to the authors, syncytial nodules perform mechanical, supporting functions in areas with closely located terminal villi [2, 5]. This was confirmed by our observations of placentas, where the percentage of the IS was increased, and the number of syncytial nodules did not differ from the norm. Other authors also observed an increase in syncytial knots in 100% of cases and considered this one of the signs of maternal malperfusion [26].

Edema of the stroma of the villi was detected in 97.3% (95% CI: 89.4%–100%) of observations and was manifested by an increase in the percentage of stroma in the villi to 71.1 [49.5; 85.1]. Additionally, edema led to a decrease in the rate of vessels in the villus to 29.9 [14.5; 51.2] against the comparison group, where the percentage of stroma and vessels was 32.6 [26.2; 39.5] and 67.4 [58.7; 73.8], respectively. The swelling of the terminal villi led to a decrease in the lumen of the intervillous channels (percentage of IS – 21.7 [12.9; 33.1] compared to 44.2 [40.3; 49.7] in the normal range) and to changes in the structure of microvilli (atrophy due to pressure), which worsened perfusion. Spherical viral particles detected by EM in the villus stroma were located extracellularly, outside the cell membrane of the fibroblast. Our data coincide with those of researchers who noted the attachment and/or budding of viral particles to cells (respiratory epithelium), indicating endocytosis or exocytosis and the presence of extracellular viral particles [15]. The authors also detected

numerous viral particles in the cytoplasm of syncytiotrophoblast and endothelium [15]. Mucoïd and fibrinoid changes in the collagen fibers of the ground substance are associated with increased permeability caused by the SARS-CoV-2 virus. The location of vessels in the terminal villi differed slightly from their location in the villi of the comparison group, where the vessels were primarily situated in the peripheral parts, ensuring adequate functioning of the vasculosyncytial membranes [3]. In our observations, the swelling of the stroma of the villi led not only to a decrease in the lumen of the vessel but also to the displacement of the vessels closer to the central parts of the terminal villi. As is generally known, this arrangement of vessels is characteristic of intermediate and terminal villi in prematurity, which is observed during the formation of chorionic villi and represents a specific feature.

The results of our study align with the findings of other authors [27] who investigated placental changes in the acute phase of COVID-19 during late gestation. These researchers also detected viral particles in the placenta, placentitis, and signs of malperfusion, even though the newborns had negative PCR tests and showed no signs of hypoxia. The obtained results may argue against the vertical transmission of SARS-CoV-2 in cases of maternal COVID-19 during late gestation, which the placental barrier function can explain.

In conclusions:

1. Pathomorphological changes in the placenta were studied primarily in the distal part of the villous chorion, which is responsible for forming vasculosyncytial membranes, in pregnant women with COVID-19 during the acute phase of the illness. These changes indicated endothelial dysfunction due to the effect of SARS-CoV-2 despite the birth of a full-term fetus with high Apgar scores and a negative PCR test.
2. Pathomorphological changes caused by endothelial dysfunction were manifested by dyscirculatory disorders, swelling of the stroma of the villi with a decrease in the lumen of the capillaries of the terminal villi of the chorion, a reduction in the percentage of free IS, and inflammatory infiltration, which led to maternal and fetal malperfusion in the placenta.
3. In our opinion, pathological changes in the structures that form the vasculosyncytial membranes were compensated by the already formed placenta, which contained a sufficient number of terminal villi and local placentitis (limited to one cotyledon).
4. Apoptotic changes in the syncytiotrophoblast and endothelium are morphological manifestations of hypoxia and energy deficiency in the placenta. These changes require further investigation in the context of the prolonged post-COVID interval in pregnant women infected with the SARS-CoV-2 virus during the second trimester.

Acknowledgements: To Zhezhera V.M, Head of the Department of Pathological Anatomy of the NSCH OHMATDYT of the Ministry of Health of Ukraine, and doctors: Chistyakova M.B., Savostikova N.L., Vystavnykh O.V.

References

1. Cindrova-Davies T, Sferruzzi-Perri AN. Human placental development and function. *Seminars in Cell & Developmental Biology* [Internet]. 2022 Nov 1;131:66–77. Available from: <https://www.sciencedirect.com/science/article/pii/S1084952122001215>
2. Burton GJ, Tham SW. Formation of vasculo-syncytial membranes in the human placenta. *J Dev Physiol*. 1992 Jul;18(1):43-7. PMID: 1287078. <https://pubmed.ncbi.nlm.nih.gov/1287078/>
3. Sankar KD, Bhanu PS, Kiran S, Ramakrishna BA, Shanthi V. Vasculosyncytial membrane in relation to syncytial knots complicates the placenta in preeclampsia: a histomorphometrical study. *Anat Cell Biol*. 2012 Jun;45(2):86-91. doi: 10.5115/acb.2012.45.2.86. Epub 2012 Jun 30. PMID: 22822462; PMCID: PMC3398179. <https://www.ncbi.nlm.nih.gov/pmc/articles/PMC3398179/>
4. Turowski G, Vogel M. Re-view and view on maturation disorders in the placenta. *APMIS*. 2018 Jul;126(7):602–12. <https://doi.org/10.1111/apm.12858>
5. Savchuk T. Pathomorphological changes of the placenta in the acute period of COVID-19 in pregnant women. *Eastern Ukrainian Medical Journal* [Internet]. 2024 Jun 24 [cited 2024 Jun 30];12(2):323-34. DOI: [https://doi.org/10.21272/eumj.2024;12\(2\):323-334](https://doi.org/10.21272/eumj.2024;12(2):323-334)
6. Burton GJ. The fine structure of the human placental villus as revealed by scanning electron microscopy. *Scanning Microsc*. 1987 Dec;1(4):1811-28. PMID: 3324327. <https://pubmed.ncbi.nlm.nih.gov/3324327/>

7. Savchuk T. Pathomorphological changes of the placenta in coronavirus disease (COVID-19) in pregnant women at 19-32 weeks of gestation. Proceeding of the Shevchenko Scientific Society. Medical Sciences, [Internet]. 2024Jun.28 [cited 2024Jun.30]; 73(1). <https://doi.org/10.25040/ntsh2024.01.16>
8. Sara S, Peter L, Ajlana L, Matts O, Francisco ON, Jan W, et al. OP003. Placental perfusion in normal pregnancy and in early and late preeclampsia: A magnetic resonance imaging study. Pregnancy Hypertension: An International Journal of Women's Cardiovascular Health. 2013 Apr;3(2):63. <https://doi.org/10.1016/j.placenta.2014.01.008>
9. Bonnet MP, Anne Alice Chantry. Placenta and uteroplacental perfusion [Internet]. Oxford University Press eBooks. Oxford University Press; 2016 [cited 2024 Apr 30]. <https://academic.oup.com/book/27881/chapter-abstract/203798546?redirectedFrom=fulltext>
10. Savchuk TV, Gychka SG, Leshchenko IV. Pathomorphological changes of the placenta in coronavirus disease (COVID 19). Patologîâ. 2021 Aug 20;18(2):128–35. <https://doi.org/10.14739/2310-1237.2021.2.231461>
11. Savchuk TV. Pathomorphological changes of the placenta in antenatal asphyxia of the fetus associated with the coronavirus disease (COVID-19) in pregnant women. Reproductive health of woman. 2023 May 31;(3):44–51. <https://doi.org/10.30841/2708-8731.3.2023.283322>
12. Savchuk T, Gychka S. Pathomorphological changes of the placenta during coronavirus disease (COVID 19) in pregnant women at 33-40 weeks of gestation. The Ukrainian Scientific Medical Youth Journal. 2024 Jun 27;146(2):119–26. DOI: [https://doi.org/10.32345/USMYJ.2\(146\).2024.119-126](https://doi.org/10.32345/USMYJ.2(146).2024.119-126)
13. Savchuk TV. [Pathomorphological Changes of the Placenta in Antenatal Asphyxia of the Fetus Associated with the Coronavirus Disease (COVID-19) in Pregnant Women]. Tuberculosis, Lung Diseases, HIV Infection (Ukraine). 2024;3:32- 39. <http://doi.org/10.30978/TB2024-3-32>. Ukrainian.
14. Beyerstedt S, Casaro EB, Rangel ÉB. COVID-19: angiotensin-converting enzyme 2 (ACE2) expression and tissue susceptibility to SARS-CoV-2 infection. European Journal of Clinical Microbiology & Infectious Diseases. 2021 Jan 3;40(5). <https://link.springer.com/article/10.1007/s10096-020-04138-6>
15. Bryce C, Grimes Z, Pujadas E, Ahuja S, Beasley MB, Albrecht R, et al. Pathophysiology of SARS-CoV-2: the Mount Sinai COVID-19 autopsy experience. Modern Pathology [Internet]. 2021 Apr 1 [cited 2021 Jun 9];1–12. Available from: <https://doi.org/10.1038/s41379-021-00793-y>
16. Nunes PR, Mattioli SV, Sandrim VC. NLRP3 Activation and Its Relationship to Endothelial Dysfunction and Oxidative Stress: Implications for Preeclampsia and Pharmacological Interventions. Cells. 2021 Oct 21;10(11):2828. doi: 10.3390/cells10112828. PMID: 34831052; PMCID: PMC8616099. <https://www.mdpi.com/2073-4409/10/11/2828>
17. Gychka SG, Brelidze TI, Kuchyn IL, Savchuk TV, Nikolaïenko SI, Zhezhera VM, et al. Placental vascular remodeling in pregnant women with COVID-19. Ito E, editor. PLOS ONE. 2022 Jul 29;17(7):e0268591. <https://doi.org/10.1371/journal.pone.0268591>
18. Aeffner F, Zarella MD, Buchbinder N, Bui MM, Goodman MR, Hartman DJ, et al. Introduction to Digital Image Analysis in Whole-slide Imaging: A White Paper from the Digital Pathology Association. Journal of pathology informatics [Internet]. 2019;10(1):9. Available from: <https://www.ncbi.nlm.nih.gov/pubmed/30984469>
19. Shackelford C, Long G, Wolf J, Okerberg C, Herbert R. Qualitative and Quantitative Analysis of Nonneoplastic Lesions in Toxicology Studies. Toxicologic Pathology. 2002 Jan;30(1):93–6. <https://journals.sagepub.com/doi/10.1080/01926230252824761>
20. Palade GE. A study of fixation for electron microscopy. Journal of Experimental Medicine [Internet]. 1952 Mar 1 [cited 2020 Oct 15];95(3):285–98. Available from: <https://rupress.org/jem/article/95/3/285/10589/A-STUDY-OF-FIXATION-FOR-ELECTRON-MICROSCOPY>
21. Reynolds ES. The use of lead citrate at high pH as an electron-opaque stain in electron microscopy. Journal of Cell Biology. 1963 Apr 1;17(1):208–12. <https://pubmed.ncbi.nlm.nih.gov/13986422/>
22. Turyanytsya SM, Korchins'ka OO, Sabova AV, Baloga OA, Petrov VO. Influence of SARS-CoV-2 acute respiratory viral disease on pregnancy and childbirth. Reprod Health Woman. 2021;2(47):15-8. <https://doi.org/10.30841/2708-8731.2.2021.232515>
23. Garg R, Agarwal R, Yadav D, Singh S, Kumar H, Bhardwaj R. Histopathological Changes in Placenta of Severe Acute Respiratory Syndrome Coronavirus 2 (SARS-Cov-2) Infection and Maternal and Perinatal Outcome in

- COVID-19. J Obstet Gynaecol India. 2023 Feb;73(1):44-50. doi: 10.1007/s13224-022-01666-3. Epub 2022 Sep 22. PMID: 36185774; PMCID: PMC9510235. <https://pmc.ncbi.nlm.nih.gov/articles/PMC9510235/>
24. Wardhana MP, Kuntaman K, Utomo B, Aryananda RA, Rifdah SN, Wafa IA, Shahnaz AA, Ningrum D, Cininta NI, Ariani G, Van Lith JM, Dachlan EG. Evidence of Placental Villous Inflammation and Apoptosis in Third-Trimester Symptomatic SARS-CoV-2 Maternal Infection. Yonsei Med J. 2024 Apr;65(4):202-209. doi: 10.3349/ymj.2023.0309. PMID: 38515357; PMCID: PMC10973560. <https://pubmed.ncbi.nlm.nih.gov/38515357/>
25. Deanfield JE, Halcox JP, Rabelink TJ. Endothelial Function and Dysfunction. Circulation. 2007 Mar 13;115(10):1285-95. <https://doi.org/10.1161/CIRCULATIONAHA.106.652859>
26. Sharps MC, Hayes DJL, Lee S, Zou Z, Brady CA, Almoghrabi Y, et al. A structured review of placental morphology and histopathological lesions associated with SARS-CoV-2 infection. Placenta. 2020 Nov;101:13-29. <https://doi.org/10.1016/j.placenta.2020.08.018>
27. Giordano G, Petrolini C, Corradini E, Campanini N, Esposito S, Perrone S. COVID-19 in pregnancy: placental pathological patterns and effect on perinatal outcome in five cases. Diagnostic Pathology. 2021 Oct 3;16(1). <https://doi.org/10.1186/s13000-021-01148-6>